The Numerical Simulation on the PBL Structure and Its Evolution over Small-Scale Concave Terrain

Shi Yong (石 勇)
Center of Space Sciences and Applied Research, Chinese Academy of Sciences, Beijing 100080
and *Jiang Weimei* (蒋维楣)
Department of Atmospheric Sciences, Nanjing University, Nanjing 210093
Received April 28, 1997; revised June 5, 1997

ABSTRACT

A high-resolution, nonhydrostatic, three-dimensional diagnostic PBL model over small-scale concave terrain was established in this paper. A two-dimensional prognostic model was developed based on the diagnostic model. The hydrostatic approximation was abandoned and the simple energy ($E-\varepsilon$) closure scheme was used in both models. Using the two models, characteristics of PBL structure and its evolution were fully studied. The main characteristic of the PBL is the circulation, and it fairly affects the distribution of the pollutant in the pit.

Key words: Small-scale concave terrain, Nonhydrostatic, Energy closure scheme, PBL numerical simulation

I. INTRODUCTION

A circulation occurs because of the special characteristic of the small-scale concave terrain when air flows over it. Previous researches and observations showed that air pollution in the small-scale concave open pit mine had much to do with the circulation and the dust concentration inside the circulation is higher than that outside. So it is much significant to study the PBL structure of small-scale concave terrain to offer some useful materials on the pollution forecasting and harnessing.

Using diagnostic model we could get some useful information under special condition and situation, such as some specific moment and stratification. But there are many factors influencing the PBL structure. We usually need to know how those factors influence the PBL and what the PBL evolution would be. It's very difficult to use the diagnostic model to meet the requirement when those factors are considered. The prognostic model can provide integrate materials about the PBL structure. But we are not sure whether the forecasting could be done in such small scale. So in this paper some attempt has been done about the prognostic probability.

Today scientists rarely pay attention to the numerical model on this side. Only some field observations and physical simulations in lab were done.

In this paper, a high-resolution, nonhydrostatic, three-dimensional diagnostic PBL model for small-scale concave terrain was established. Then a same high-resolution, two-dimensional prognostic model was developed. Using these two models, some specific PBL structures and their whole evolution process are simulated.

II. ESTABLISHMENT OF THE MODEL

1. *Basic Equations*

Terrain-following coordinate is adopted in the models in order to consider the influence

of the terrain. So the basic equations in the terrain-following coordinate can be written as follows (Pielke, 1984):

$$\frac{du}{dt} = f(v - v_g) - \theta\frac{\partial \pi'}{\partial x} - \theta\frac{z^* - h_d}{h_d - z_g}\frac{\partial z_g}{\partial x}\frac{\partial \pi'}{\partial z^*} + \frac{\partial}{\partial x}(K_{mh}\frac{\partial u}{\partial x}) + \frac{\partial}{\partial y}(K_{mh}\frac{\partial u}{\partial y}) + (\frac{h_d}{h_d - z_g})^2\frac{\partial}{\partial z^*}(K_{mz}\frac{\partial u}{\partial z^*}) , \quad (1)$$

$$\frac{dv}{dt} = -f(u - u_g) - \theta\frac{\partial \pi'}{\partial y} - \theta\frac{z^* - h_d}{h_d - z_g}\frac{\partial z_g}{\partial y}\frac{\partial \pi'}{\partial z^*} + \frac{\partial}{\partial x}(K_{mh}\frac{\partial v}{\partial x}) + \frac{\partial}{\partial y}(K_{mh}\frac{\partial v}{\partial y}) + (\frac{h_d}{h_d - z_g})^2\frac{\partial}{\partial z^*}(K_{mz}\frac{\partial v}{\partial z^*}) , \quad (2)$$

$$\frac{dw}{dt} = g\frac{\theta'}{\theta_m} - \theta\frac{z^* - h_d}{h_d - z_g}\frac{\partial \pi'}{\partial z^*} + \frac{\partial}{\partial x}(K_{mh}\frac{\partial w}{\partial x}) + \frac{\partial}{\partial y}(K_{mh}\frac{\partial w}{\partial y}) + (\frac{h_d}{h_d - z_g})^2\frac{\partial}{\partial z^*}(K_{mz}\frac{\partial w}{\partial z^*}) , \quad (3)$$

$$\frac{d\theta}{dt} = \frac{\partial}{\partial x}(K_{\theta h}\frac{\partial \theta}{\partial x}) + \frac{\partial}{\partial y}(K_{\theta h}\frac{u}{\partial y}) + (\frac{h_d}{h_d - z_g})^2\frac{\partial}{\partial z^*}(K_{\theta z}\frac{\partial \theta}{\partial z^*}) \quad (4)$$

$$\frac{\partial u}{\partial x} + \frac{\partial v}{\partial y} + \frac{\partial w^*}{\partial z^*} - \frac{1}{h_d - z_g}(u\frac{\partial z_g}{\partial x} + v\frac{\partial z_g}{\partial y}) = 0 , \quad (5)$$

$$z^* = h_d\frac{z - z_g(x,y)}{h_d - z_g(x,y)} , \quad (6)$$

where $z_g(x,y)$ is the terrain function, and h_d is the total height of the model.

The simple energy $(E-\varepsilon)$ closure scheme is used in these two models (Detering et al., 1985; Duynkerke, 1988). The prognostic equations of turbulence energy (E) and dissipation rate (ε) must be introduced as below:

$$\frac{dE}{dt} = \left(\frac{h_d}{h_d - z_g}\right)^2 K_{mz}\left[\left(\frac{\partial u}{\partial x}\right)^2 + \frac{\partial v}{\partial y}\right] + \frac{h_d}{h_d - z_g}\frac{g}{\theta}K_{\theta h}\frac{\partial \theta}{\partial z} + \frac{\partial}{\partial x}(\frac{K_{mh}}{\sigma_E}\frac{\partial E}{\partial x}) + \frac{\partial}{\partial y}(\frac{K_{mh}}{\sigma_E}\frac{\partial E}{\partial y}) + (\frac{h_d}{h_d - z_g})^2\frac{\partial}{\partial z^*}(\frac{K_{mz}}{\sigma_E}\frac{\partial E}{\partial z^*}) - \varepsilon , \quad (7)$$

$$\frac{d\varepsilon}{dt} = \frac{\partial}{\partial x}(\frac{K_{mh}}{\varepsilon_\sigma}\frac{\partial \varepsilon}{\partial x}) + (\frac{h_d}{h_d - z_g})^2\frac{\partial}{\partial z^*}(\frac{K_{mz}}{\sigma_\varepsilon}\frac{\partial \varepsilon}{\partial z^*}) + \frac{\partial}{\partial y}(\frac{K_{mh}}{\sigma_\varepsilon}\frac{\partial \varepsilon}{\partial y}) + C_{1\varepsilon}\frac{\varepsilon}{E}\{(\frac{h_d}{h_d - z_g})^2 K_{mz}[(\frac{\partial u}{\partial x})^2 + (\frac{\partial v}{\partial y})^2] - (1 - C_{3\varepsilon})\frac{g}{\theta}\frac{h_d}{h_d - z_g}K_{\theta z}\frac{\partial \theta}{\partial z}\} - C_{2\varepsilon}\frac{\varepsilon^2}{E} , \quad (8)$$

where $K_{mh} = K_{\theta h}$, and $K_{mz} = K_{\theta z} = C_\mu\frac{E^2}{\varepsilon}$, $C_\mu = 0.09$, $\sigma_E = 1.0$, $\sigma_\varepsilon = 1.3$, $C_{1\varepsilon} = 1.44$, $C_{2\varepsilon} = 1.92$, and $C_{3\varepsilon} = 1.0$ when stable, $C_{3\varepsilon} = 0.0$ when unstable.

2. *Three-Dimensional Diagnostic Model*

Based on the basis equations, closure scheme and some suitable initial and boundary conditions, a three-dimensional diagnostic model can be established. In this paper the PBL

structure under neutral stratification is simulated and some useful information gotten.

3. *Two-Dimensional Prognostic Model*

In order to consider the ground temperature's influence on the free atmosphere, a prognostic equation of ground temperature (T_g) must be introduced. Blacdar (1979) put forward an energy budget equation to decide ground temperature

$$C_g \frac{\partial T_g}{\partial t} = R_n - H_m - H_s - H_l \ , \tag{9}$$

where R_n is net radiative flux, H_s the sensible heat flux, H_e the latent heat flux, H_m the heat flow into the substrate and C_g the thermal capacity of the slab per unit area. In this paper, C_g equals $12 \times 10^4 \mathrm{JM^{-2}K^{-1}}$.

a. *Net radiative flux* R_n

$$R_n = Q_s + I\uparrow + I\downarrow \ , \tag{10}$$

where Q_s, the amount of solar radiation absorbed by the ground, is approximately written as

$$Q_s = S_0(1-A)\cos\xi\tau_s^{\sec\xi} \ , \tag{11}$$

where S_0 denotes the intensity of solar radiation at the top of the atmosphere, A the ground albedo, ξ the solar zenity angle, τ_s the atmospheric transmissivity, and

$$\cos\xi = \sin\varphi\sin\delta + \cos\varphi\cos\delta\cos\omega \ , \tag{12}$$

in which φ represents the latitude of the location, δ the solar declination, and ω the local hour angle of the sun.

As we know that the slope and direction of the concave terrain fairly affect the distribution of the solar radiation on the ground. Fu Baopu (1982) suggested that the amount of solar radiation absorbed by the slope ground is

$$Q_{\alpha,\beta} = S_0[\sin h\cos\alpha + \cos h\cos(B-\beta)\sin\alpha] \ , \tag{13}$$

where α is the slope, β the direction, h the solar zenity angle, and B the solar azimuth.

Fu (1982) also gave some astronomy formulas as

$$\cos h\cos B = -\sin\delta\cos\varphi + \cos\delta\sin\varphi\cos\omega \ , \tag{14}$$

$$\cos h\sin b = \cos\delta\cos\omega \ ,$$

and if

$$\begin{aligned} u &= \sin\varphi\cos\alpha - \cos\varphi\sin\alpha\cos\beta \ , \\ v &= \cos\varphi\cos\alpha + \sin\varphi\sin\alpha\cos\beta \ , \end{aligned} \tag{15}$$

then

$$Q_{\alpha,\beta} = S_0(u\sin\delta + v\cos\delta\cos\omega + \sin\beta\sin\alpha\cos\delta\cos\omega) \ . \tag{16}$$

The integrated solar short-wave radiation flux in which the slope and direction of the fields and the solar azimuth are considered is written as

$$Q_{\alpha,\beta} = S_0(1-A)(u\sin\delta + v\cos\delta\cos\omega + \sin\beta\sin\alpha\cos\delta\cos\omega)\tau_s^{\sec\xi} \ , \tag{17}$$

in which $\sec\xi = \frac{1}{\cos\xi}$ and $\cos\xi = \sin h_{\alpha,\beta}$.

In this model we simply cut off a section of the actual terrain as the simulation domain. On southern slope $\beta = 0$ and northern slope $\beta = pi$. The form of the slope α can be shown as

$$\alpha = \mathrm{arctg}[(\frac{\partial Z_g}{\partial x})^2 + (\frac{\partial Z_g}{\partial y})^2]^{\frac{1}{2}} , \tag{18}$$

where $Z_g(x,y)$ is the terrain function.

The net longwave radiation is divided into incoming $I\downarrow$ part which is specified a constant 275 $JM^{-2}S^{-1}$ (Daling Zhang, 1982) and outgoing $I\uparrow$ part,

$$I\uparrow = \varepsilon\alpha T_g^4 , \tag{19}$$

where ε is the slab emissivity, σ is the Stefen–Boltzman constant, and T_g the ground temperature which is obtained from the ground temperature prognostic equation.

b. *Sensible heat and latent heat flux*

The sensible heat flux H_s is of the form.

$$H_s = -C_p \rho u_* T_* , \tag{20}$$

in which ρ is the air density near ground surface, C_p the specific heat at constant pressure, u_* the friction velocity, T_* the friction temperature.

The latent heat flux H_l can be written as,

$$H_l = H_s / Bw , \tag{21}$$

where $Bw = 0.5$.

c. *Heat flow into the substrate* H_m

The transfer of heat due to molecular conduction is calculated from the equation

$$H_m = C_g K_m (T_g - T_m) , \tag{22}$$

where K_m is the heat transfer coefficient expressed as $K_m = 1.18\omega$ and T_m is the temperature of the substrate (Blackadar, 1979).

4. *Boundary Condition*

It's important to select suitable lower boundary conditions. At the height of roughness u,v,w are equal to 0. θ is calculated as

$$\theta_0 = \theta_g + 0.0962(T_* / \kappa)(u_* z_0 / \nu)^{0.45} \tag{23}$$

to realize the coupling of the ground temperature (T_g) and free atmosphere temperature (T_0). The first level of the model is selected to be the lower boundary where the variables are specified by the ground layer profile formulas (Businger, 1971).

The same scheme is used in our diagnostic model.

5. *Initial Conditions*

The initial velocity was assumed to distribute as power index ($P = 0.25$) under 300 m and evenly up 300 m in the diagnostic model. The neutral stratification was selected to be the initial conditions of potential temperature in the diagnostic model, which would never change

and alter during the simulation process.

In the prognostic model the intial velocity is as same as that in diagnostic model. And θ is defined initially as

$$\theta(x, z^*) = 293k, z^* \leqslant 1500 \text{ m},$$
$$\theta(x, z^*) = 293 + 0.01(z^* - 1500), z^* > 1500 \text{ m}, \quad (24)$$

the initial condition about v,w is $v = w = 0$.

6. *Simulation Domain and Mesh*

The actual terrain of one concave open pit mine which covers 2 km × 2 km is used as the simulation domain. The horizontal meshes are designed to be 31 × 31 and the minimum grid size was 60 m. The height of the model is about 5000 m which is divided into 19 layers. The first layer is 5 m high away from the ground.

III. SIMULATION RESULTS

1. *Analysis of the PBL Structure under Neutral Stratification*

To demonstrate the PBL structure of the small-scale concave terrain, a representative neutral stratification steady-state PBL over the terrain is simulated here.

Fig. 1 is the velocity profile at $y = 970$ m vertical section. When the air flows into the pit, the velocity immediately decreases because of the block of the terrain. At the same time, an obvious back-flow appears on the ground of the pit which is nearly 80 m high and 300 m wide. It will rapidly restore to some extent corresponded to the amount at upper reaches as soon as flowing outside the pit. The maximum velocity is about −1.5 m / s. The profiles at $y = 610$ m and $y = 1330$ m section where the terrain is flatter and more shallow show that the back flow is not strong in comparison to $y = 970$ m.

Fig. 2 shows the u and w components of the wind at $y = 970$ m section, from this we can see that there exists a clear circulation on the top of which is covered with straight flow. Inside

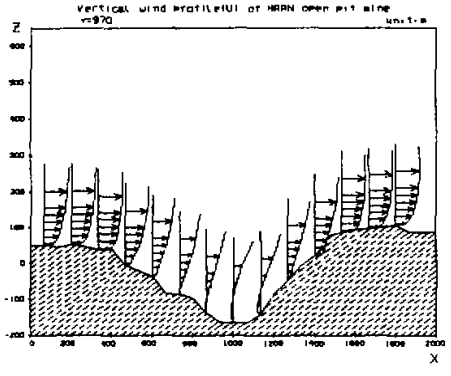

Fig.1. Horizontal velocity profile at $y = 970$ m section.

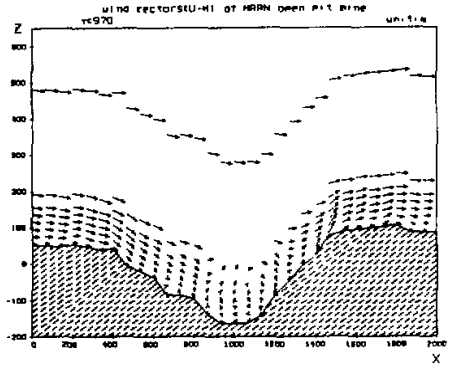

Fig.2. u and w components of winda at $y = 970$ m section.

the circulation there is a strong air convection. The circulation is about 120 m high and 600 m wide. The circulation is not formed at $y=670$ m and $y=1330$ m section.

Fig.3 shows u and v components of the wind at $z=-100$ m. The obvious back flow indicates that the block of the terrain is very strong at this section.

The major characteristic of the PBL structure over the small-scale concave terrain is the existence of the circulation. The circulation has reversing, low-velocity and sealing structure.

2. *Evolution of the PBL Structure*

The prognostic model was run for 24h started from 8:00 this day to 8:00 next day to simulate the evolution of the PBL. Along with the sun rising, ground surface is heated and a distinct circulation is induced at 11 o'clock (Fig. 4). There is an obvious rising airflow area on the lee side. The air sinks on the top of the pit and reverses on the windward side. The circulation which is nearly 600 m high covers about 700 m in horizontal direction. The horizontal velocity component of the sinking airflow gradually increases on the top of the windward side and finally turns to blow straight. This circulation is larger and deeper than that simply brought out by the block from the terrain shown in Fig. 2. The strong rising and sinking airflow accelerates the air mixing in the circulation, which leads to the well-distribution of each physical variable.

The circulation is weakened and then slowly disappears in the afternoon because the heating of the sun gradually subsides. At 14 o'clock (Fig.5), there is a weakened circulation, 250 m high and 500 m wide, which comes to disappear at 16 o'clock (Fig.6) and leaves only straight airflow in the pit. After 18 o'clock, a stable stratification is formed near the ground layer by the remarkable dropping of the soil temperature. The mountain slope and the air in contact with it cool off more rapidly than the free atmosphere, and this different heating will generate a circulation called the mountain wind soon after the sunset. About 2 hours later the wind reaches its maximum speed (Fig.7). At 22 o'clock there is large scope of wind shadow or small-speed wind area near the ground, approximately remaining steady throughout the night until sunrise (Fig.9).

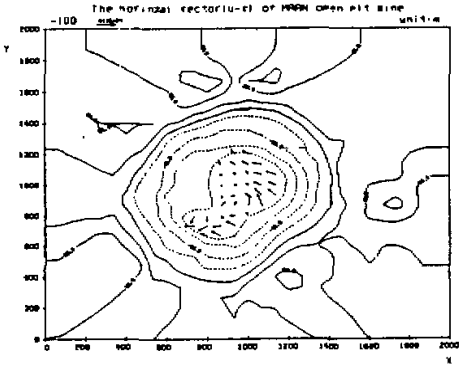

Fig.3. u and v components of wind at $y=970$ m section.

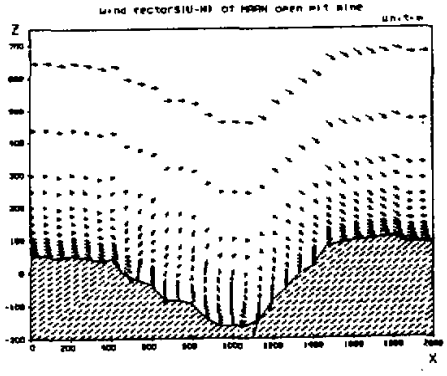

Fig.4. u and w components of wind at 11:00.

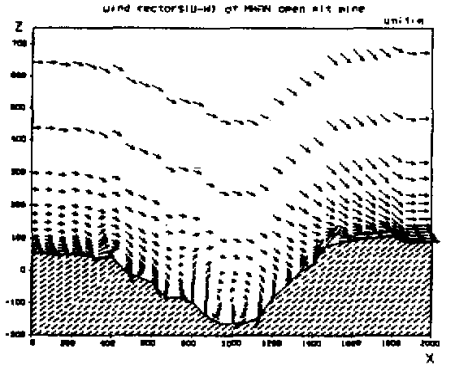

Fig.5. u and w components of wind at 14:00.

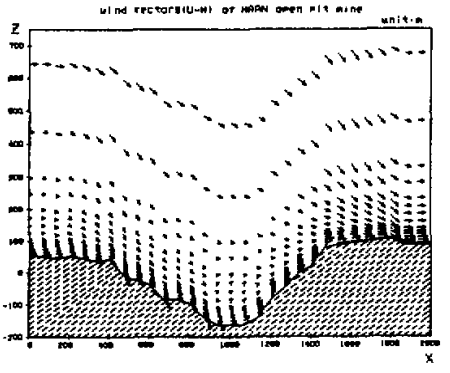

Fig.6. u and w components of wind at 16:00.

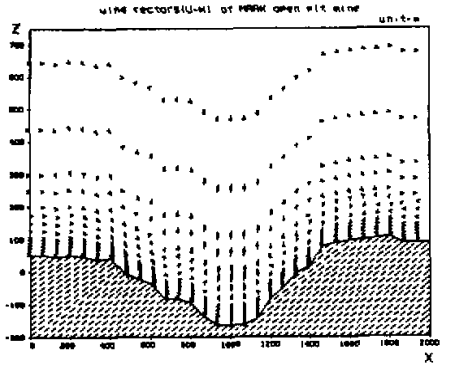

Fig.7. u and w components of wind at 20:00.

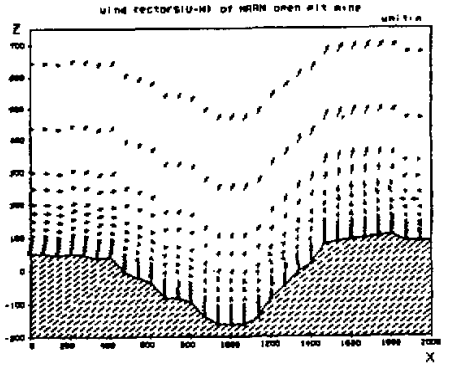

Fig.8. u and w components of wind at 22:00.

IV. CONCLUSION

The results indicate that both the diagnostic model and the prognostic model can simulate the small-scale PBL problem over complex terrain.

The most important characteristic about the PBL structure is the circulation which has a reversing, slow and sealing structure. The thermal forcing effect and the terrain blocking effect seriously influence the evolution of the structure, which would lead to different pollution situations. We could foretell the distribution of the pollutant relying on those results shown above.

All the work is somewhat an attempt to the study of such small-scale over complex terrain, especially the probability of the prediction about the prognostic model. The results are waiting for being verified by some observation materials.

REFERENCES

Blackadar A.K. (1979), High Resolution Models, The Planetary Boundary Layer, *Advances in Environmental Science and Engineering*, **1(1):** Pfafflin and Ziegler, Eds, Gordon and Breach Sci. Pub., New York, 50–85.

Businger, J.A., Wyngaard, J.C. et al. (1971), Flux-Profile Relationships in the Atmospheric Surface Layer, *J.A.S.*, **28:** 181–189.

Detering H.W. and Etling D. (1985), Application of the ($E-\varepsilon$) Turbulance Model to the Atmospherical Boundary Layer, *Boundary Layer Meteor.*, **33:** 113–133.

Duynkerke P.G. (1988), Application of the ($E-\varepsilon$) Turbulance Closure Model to the Neutral and Stable Atmospheric Boundary Layer, *J.A.S.*, **44:** 43–46.

Fu Baopu (1983), Mountain Region Climate, Science Press, Beijing.

Pielke R.A. (1984), Mesoscale Meteorological Modeling, Academic Press.

Zhang Dalin, Richard A. Anthes (1982), A High-Resolution Model of the Planetary Boundary Layer–Sensitivity Tests and Comparisons with SESAME-79 Data, *Journal of Applied Meteor.*, **21:** 1594–1609.